Regular, irregular, and scarred wave functions in the two-center shell model

Debabrata Biswas
Theoretical Physics Division, Central Complex, Bhabha Atomic Research Centre, Bombay 400 085, India

Santanu Pal and A. K. Chaudhuri
Variable Energy Cyclotron Centre, 1/AF Bidhan Nagar, Calcutta 700 064, India
(Received 10 September 1991; revised manuscript received 31 December 1991)

The two-center shell-model potential admits a two-component eigenfunction due to the presence of the spin-orbit coupling. We carry out a detailed numerical study of its variation with the shape of the potential and also investigate the applicability of the criteria commonly used to distinguish regular and irregular states in systems that possess a clear classical analog. Our results corroborate similar studies on spectral fluctuations. The occurrence of scarred states and a Gaussian amplitude distribution strongly indicate the presence of an underlying classical dynamics. Moreover, since the spin-up and spin-down spatial components of each eigenfunction are significantly dissimilar, there seem to be two sets of closed orbits that give rise to the same spectrum but influence the wave functions in different ways.

PACS number(s): 03.65.Sq, 03.65.Ge, 05.45.+b

I. INTRODUCTION

The past decade has seen considerable progress in the study and characterization of semiclassical states in quantum systems with both integrable and nonintegrable classical analogs [1]. Most of the work has been confined to the statistical properties of energy levels, and it is now firmly established that there exists an intimate relationship between the spectral fluctuations and the underlying classical dynamics [2,3]. Almost all theoretical results in this direction [4,5] are based on the periodic-orbit theory (POT) [6–8], which provides a connection between the semiclassical density of states and the classical periodic orbits of the system. Together with the "principle of uniformity" developed by Hannay and Ozorio de Almeida [9], it has been possible to arrive at analytical forms for various measures on the spectrum for integrable as well as chaotic systems [2,4,5]. In the latter case the results are identical to the predictions of random matrix theory for the Gaussian orthogonal ensemble [10] when the corresponding classical system possess time reversal invariance.

Periodic orbits also show up dramatically in the eigenfunctions of systems that are classically nonintegrable. The phenomenon was observed by Heller in the Bunimovich stadium billiard where a number of eigenfunctions both at low and high energies were found to be localized on and around a single (or a few) periodic orbits of the system [11]. They are now referred to as "scarred" states and have been observed in other systems as well [12]. Bogomolny [13] and subsequently Berry [14] have been able to use the POT to arrive at expressions for the averaged intensity ($|\Psi(q)|^2$) and the Wigner function, respectively. Their analysis also explains some of the finer observations on scarred states. The work of Eckhardt, Hose, and Pollack [15] on the quartic potential is also significant since it clearly brings out the importance of adiabatic stability (of periodic orbits in the Lyapunov sense) in the localization process.

There are other manifestations of periodic orbits in eigenfunctions as well. Scarred states such as those observed by Heller are more of an exception. In general, the eigenfunctions are quite complicated when the underlying classical dynamics is chaotic. Recently Biswas, Azam, and Lawande [16] have used the periodic-orbit approach to show that generic eigenfunctions do indeed have a limiting amplitude distribution which in fact closely approximates a Gaussian. This corroborates the predictions of Berry [17] arrived at by using an infinite superposition of plane waves with equal wave-vector magnitude but random phase and direction. Incidentally this model also leads to a spatial correlation function that is isotropic and has a Bessel-function dependence [17]. These properties together with the nodal pattern and the phenomenon of contour splitting [18] are some of the important criteria for distinguishing an irregular eigenfunction from one that is regular.

Unlike spectral statistics, studies on wave functions have largely been confined to systems that have a clear classical analog. How do eigenfunctions behave when the system is purely quantum mechanical (e.g., spin dependent)? Are the properties mentioned above useful in distinguishing regular and irregular states in such cases? One of the basic motivations of the current work is to answer this and questions related to the role of periodic orbits, if any.

In the following we shall study the single-particle states in the two-center shell model. It describes a system of two colliding nuclei and is parameterized by the separation R. The presence of the spin-orbit potential leads to a two-component eigenfunction. Among other things, we shall study the evolution for the adiabatic states as a function of R and look for a transition from regularity (at large R) to irregularity (intermediate R) and back again to regularity ($R \rightarrow 0$). This expectation is based on recent studies on spectral statistics [19,20] which reveal a Poisson–Wigner-like–Poisson transition in the nearest-neighbor level spacing distribution. For systems with a

classical limit, this immediately implies a regular-irregular-regular transition in generic eigenfunctions. Does such a thing happen in the present case as well?

The paper is organized along the following lines. In Sec. II we discuss the two-center shell potential and briefly describe the numerical scheme used to arrive at the eigenfunctions. Studies on nodal patterns and contour plots are presented in Sec. III for various values of R and at low as well as high energies. We also look at the amplitude distribution for a typical regular and irregular wave function and use the phenomenon of contour splitting to study the "surface roughness." Section IV is devoted to scarred states while the concluding section summarizes our results.

II. THE TWO-CENTER POTENTIAL

The two-center potential has often been used to model shape transitions in heavy ion collisions. The total Hamiltonian of a single particle in the combined field of two axially symmetric harmonic oscillators centered at $z_1<0$ and $z_2>0$ (the position of the barrier is at the origin) joined smoothly by a neck (Fig. 1) and with a spin-orbit potential is given as [21]

$$H=T+U+U_{\rm SO} \tag{1}$$

where $U=U_{\rm HO}+U_{\rm neck}$ and

$$U_{\rm HO}=U(\omega_{\rho 1},\omega_{\rho 2},\omega_{z1},\omega_{z2};\rho,z)$$
$$=\begin{cases}\frac{1}{2}M\omega_{\rho 1}^2\rho^2+\frac{1}{2}M\omega_{z1}^2(z-z_1)^2 & \text{for } z<0\\ \frac{1}{2}M\omega_{\rho 2}^2\rho^2+\frac{1}{2}M\omega_{z2}^2(z-z_2)^2 & \text{for } z>0\ ,\end{cases} \tag{2}$$

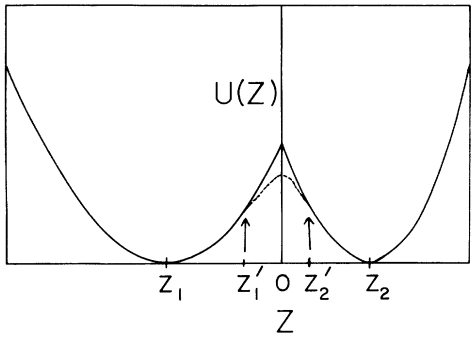

FIG. 1. The two-center oscillator potential along the z axis. The two centers are at z_1 and z_2 and the barrier is at the origin. The barrier heights with (dotted line) and without (full line) the neck potential are U_1 and U_2, respectively, as used in the text.

ρ and z being the cylindrical coordinates. The above potential is essentially characterized by

$$R=z_2-z_1\ ,$$
$$Q=\omega_{\rho 2}/\omega_{\rho 1}\ , \tag{3}$$
$$\delta=\omega_{z1}/\omega_{\rho 1}=\omega_{z2}/\omega_{\rho 2}\ ,$$

giving $z_1=-QR/(1+Q)$ and $z_2=R/(1+Q)$. The neck potential joining the two oscillators of Eq. (2) is defined as [21]

$$U_{\rm neck}=\begin{cases}\frac{1}{2}M[d_1\omega_{z1}^2(z-z_1)^2+g_1\omega_{\rho 1}^2\rho^2](z-z_1')^2\theta(z-z_1') & \text{for } z<0\\ \frac{1}{2}M[d_2\omega_{z2}^2(z-z_2)^2+g_2\omega_{\rho 2}^2\rho^2](z-z_2')^2\theta(z_2'-z) & \text{for } z>0\end{cases} \tag{4}$$

for $z_1'<0<z_2'$. The parameters of Eq. (4) are obtained from the smooth matching conditions of the potential and are given as

$$\epsilon=U_1/U_2\ ,$$
$$z_i'=z_i(1-\epsilon)/\epsilon\ ,$$
$$d_i=-\epsilon^2/[(1-\epsilon)z_i^2]\ , \tag{5}$$
$$g_1=\epsilon^2(Q^2-1)(Q+1)/[(1-\epsilon)^2QR^2]\ ,\quad g_2=-g_1/Q\ .$$

The spin-orbit potential is evaluated in the same way as in Ref. [22].

For a given R, Q, ϵ, and δ, only one of the frequencies remains to be fixed for a complete description of the model. Considering a system of A nucleons, we shall obtain the frequency $\omega_{\rho 1}$ by requiring [22] the volume under the equipotential surface $V_0=M\omega_0^2R_0^2/2=W_0=(4\pi/3)R_0^3$ where $R_0=1.2249\ A^{1/3}$ fm and $\hbar\omega_0=41$ MeV $A^{-1/3}$.

In what follows, we shall consider an $A=260$ system with $\delta=1$ and $\epsilon=0.8$. The asymptotic value of Q is taken as 1.1695 which corresponds to an asymptotic mass asymmetry of 1.6, thereby placing two nuclei of masses 160 and 100 at z_1 and z_2, respectively, for large separations. We shall be concerned with the neutron single-particle levels in the following calculations.

In the absence of neck and spin-orbit potentials, the system is clearly separable and can be assigned good quantum numbers. The eigenfunctions are thus regular as one would expect. The introduction of the neck potential leads to nonseparability in the region $z_1'<z<z_2'$. Our numerical investigations show that the nature of quantum-mechanical energy eigenfunctions does not change drastically even at this stage. The presence of the spin-orbital potential, however, has significant effects. The eigenfunctions ψ_n of the time-independent Schrödinger equation

$$H\psi_n=E_n\psi_n \tag{6}$$

now have two components and are of the form

$$\psi_n = \phi_n^1(\rho,z)|\uparrow\rangle + \phi_n^2(\rho,z)|\downarrow\rangle \ . \tag{7}$$

Thus each ϕ_n must be studied separately.

We have obtained the eigenfunctions by diagonalizing the Hamiltonain in a basis given in Ref. [22]. Numerical errors are under control and states satisfy the orthonormality requirement to a good accuracy.

III. REGULAR AND IRREGULAR STATES

A. Nodal patterns and contour plots

Nodal curves contain a considerable amount of information and have long been studied in theoretical acoustics. They have found wide applicability in quantum mechanics as well [23]. The terms "regular" and "irregular" have in fact come to be associated with the nodal pattern itself. Heller [24] has, however, demonstrated that an irregular-looking nodal plot is not sufficient for quantum mechanics to "mimic" classical chaos since a superposition of even six cosine wave with random phase and direction is sufficient to generate complex patterns. The detailed study of Biswas and Jain [25] on a pseudointegrable system shows that irregular nodal curves occur even when the classical dynamics is nonchaotic (in the Lyapunov sense) but nonintegrable. The corresponding spectral statistics, however, does seem to have a close link with the eigenfunction categorized in this sense and it has been observed [25] that a sequence of states with a large irregular fraction leads to fluctuations that are far from Poissonian.

We present here our results from a typical eigenfunction at intermediate energies (Fig. 2) for various values at the separation R. The change in nodal pattern is similar to the transition observed in spectral fluctuations [19]. At large separations (R =21 fm) the pattern is more or less regular but becomes quite complex as the nuclei come closer (12–7 fm). As the separation becomes smaller still, the nodal curves once more become regular.

Figure 3 shows the positive contours of each component for identical separations. It gives a clearer picture and helps remove some ambiguities. The spin-up part at R =21 fm, for example, has a negligible amplitude on the right (<0.01) where nodal patterns show relatively greater complexity. On the left, the contour patterns are regular as expected. Thus nodal patterns alone are insufficient and should be viewed in conjunction with the contour plots. As far as the regular-irregular-regular transition is concerned, the plots in Fig. 3 corroborate our earlier observations.

Figure 4 shows plots (nodal as well as contour) of a typical wave function at low energy for a sufficiently larger separation (we have computed at R =21 fm). The wave function is localized to the left and the patterns are regular. At higher energies, however, the wave function becomes delocalized and exhibits irregularity.

An analysis neglecting the spin-orbit potential is clearly inadequate. On the other hand, the spatial wave functions associated with the spin-up or -down cases, which are otherwise coupled through the spin-orbit interaction, do have definite features which appear to evolve independently in the regular-irregular-regular transition. This would indicate that the spin-orbit interaction is also weak enough to respect certain gross features of the potential $U(\rho,z)$ for the particular eigenstate considered above. [For example, the state in Fig. 4 is much below the barrier of the potential $U(\rho,z)$ and hence the localization mentioned above could still be due to this confining mechanism. A similar localization effect for the 80th state at the same separation (see Fig. 3) where the eigenenergy is just above the barrier height suggests that the spin-orbit coupling might in fact push up the effective barrier height marginally.] Recalling that the spin-orbit

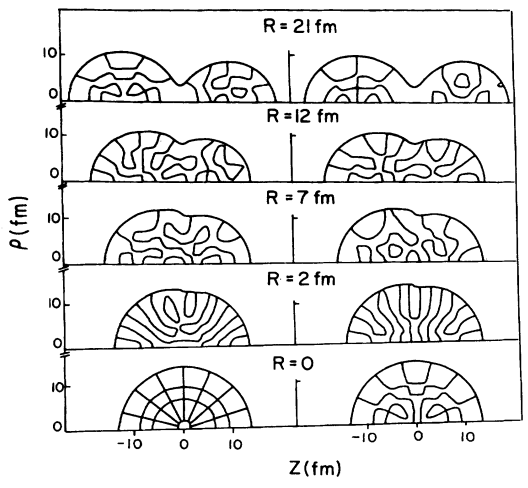

FIG. 2. Typical nodal plots at different separations within the classically allowed region defined by the smooth outer line. The energy eigenvalue for the 80th state (N =80) at R =21, 12, 7, 2, and 0 fm are 79.54, 82.80, 86.39, 86.90, and 87.24 MeV, respectively.

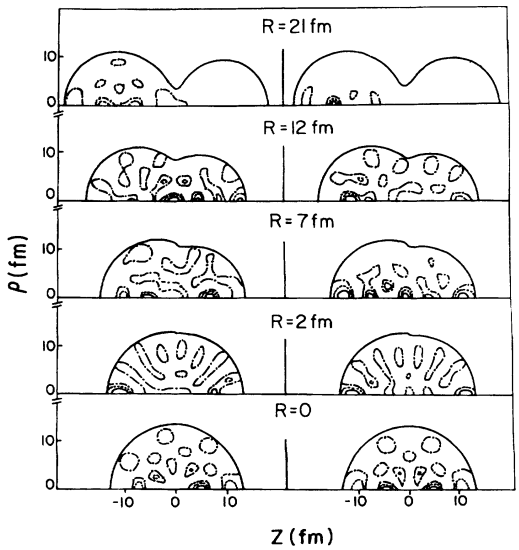

FIG. 3. Contour plots of the eigenfunction considered in Fig. 2. The full line is for (ψ=)0.1, dashed line for 0.05, and dashed-dotted line for 0.01.

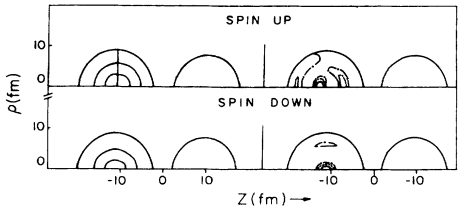

FIG. 4. Large separation behavior (regular) or nodal curves and contour plots for $N=38$ at $R=21$ fm. The eigenenergy 53.98 MeV is below the barrier.

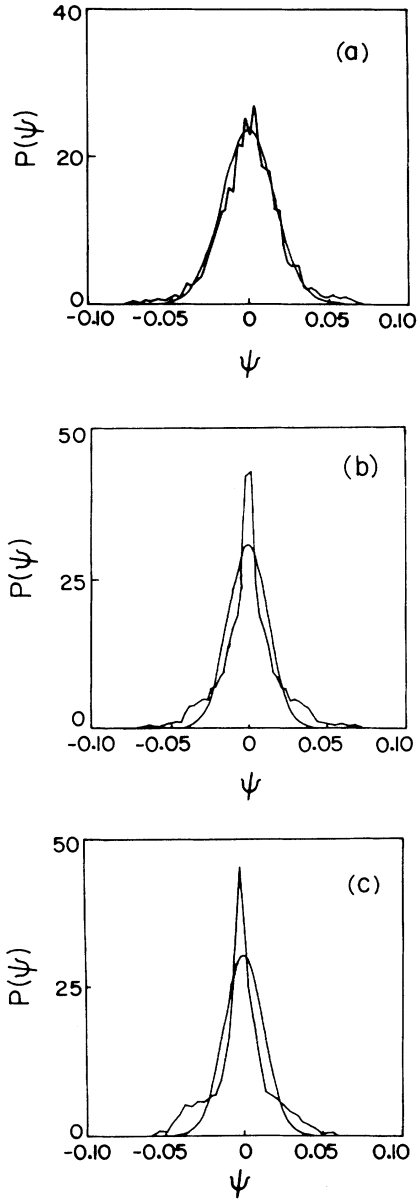

FIG. 5. The amplitude distribution $P(\psi)$ for (a) an irregular state at $R=19.6$ fm, $N=106$, spinup, $E=102.46$ MeV; (b) a regular state at $R=0$, $N=106$, spin down, $E=103.47$ MeV; and (c) a localized state at $R=4$ fm, $N=104$, spin down, $E=101.88$ MeV. The best-fit Gaussian is also shown in each case.

potential is a state-dependent one, it is not possible at the moment to conclude that this observation is true for other eigenstates as well. This aspect is currently under investigation.

B. The amplitude distribution $P(\psi)$

The amplitude distribution is increasingly being recognized as an important criterion for distinguishing regular and irregular eigenfunctions. It was first suggested by Berry [17] that the distribution $P(\psi)$ should be Gaussian when the underlying classical dynamics is chaotic. The ideas were based on the eikonal theory and the eigenfunction was represented as an infinite sum of plane waves with equal wave-vector magnitude but random phase and direction. By the central-limit theorem then, ψ is a Gaussian random variable. The representation, however, has inadequacies. Biswas, Azam, and Lawande [16] have recently used the periodic-orbit approach to argue that there exists a limiting distribution which closely approximates a Gaussian when the system is classically chaotic. Such a distribution has also been observed by Biswas and Jain [25] in (nonchaotic) pseudointegrable systems. As in the case of the intricate nodal patterns, a Gaussian amplitude distribution is thus an indicator of irregularity in the eigenfunction but does not necessarily imply a chaotic classical dynamics.

For the numerical results that we present here, a total of 4500 points have been sampled in the classically allowed domain [determined by the potential $U(\rho,z)$] to evaluate $P(\psi)$. Figure 5(a) shows the amplitude distribution of a typical irregular wave function at $R=19.6$. We have considered the spin-up component of the 106th state which lies sufficiently above the barrier. The corresponding nodal plot is shown in Fig. 6. The wave function is clearly irregular and the corresponding amplitude distribution approximates a Gaussian rather well.

A typical regular component at $R=0$, however, shows quite the opposite behavior [Fig. 5(b)]. The distribution $P(\psi)$ shows a sharp deviation from a Gaussian especially due to the peak at zero. This is similar to observations on regular states in other system as well [25].

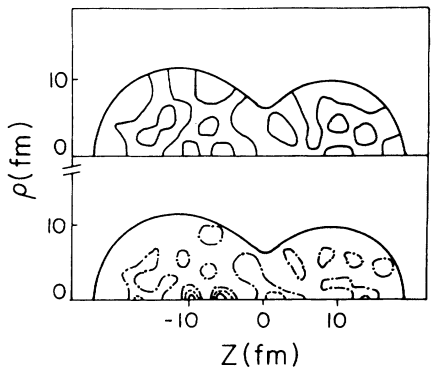

FIG. 6. Contour plot of an irregular state at $R=19.6$ fm, $N=106$, spin up, $E=102.46$ MeV. The corresponding amplitude distribution is shown in Fig. 5(a).

The spin-down component of the 104th state at $R=4$ fm has an intermediate nature (see Fig. 11). The wave function appears to be localized in narrow regions. The corresponding amplitude distribution [Fig. 5(c)] shows sharp deviations from a Gaussian as before. Further details of such states are given in the following section.

C. Contour splitting

While nodal curves (or sections) provide a visual picture of the degree of irregularity in the wave function at a given height ($\psi=z$), the degree of "surface roughness" can be visualized from the degree of "contour splitting" as shown by Biswas, Azam, and Lawande [18]. A rough surface (to the extent allowed by the second-order partial differential equation) manifests itself as a splitting of contours when sections at successive heights are taken. This information in a sense is contained in the amplitude distribution as well. The Gaussian distribution implies that the number of points in configuration space at a given small positive or negative value (which is a measure of the length of the contours at that height) is nearly the same as the number at $\psi=0$. This can only occur if the individual contours (at $\psi=0$) split into two or more as $|\psi|$ increases from zero. Further, due to the random spatial distribution of the isolated periodic orbits (in systems where a clear classical analog does exist), this phenomenon is also likely to occur away from zero. The plot of $P(\psi)$ would then have sharp spikes superimposed on the Gaussian (for more details see Biswas, Azam, and Lawande [18]).

A clear example of contour splitting is the spin-down component of the 80th state at $R=12$ fm (Fig. 3). The contour near $\rho=0$ towards the left center is a clear example. While the phenomenon is totally absent in the regular states, there are irregular states (in the nodal sense) as well where splitting does not occur. The criterion thus identifies the degree of irregularity.

IV. SCARS OF PERIODIC ORBITS?

Scars have so far been observed in systems which possess a clear classical analog. In such cases, the periodic orbits along with the available phase-space volume determine the individual eigenfunctions (at least in an averaged sense) when the system is chaotic [13,14]. The contribution of each orbit, however, depends sensitively on the energy and in general an eigenstate is quite complex. Exceptional states are, however, dominated by a single (or a few) periodic orbit and they are referred to as "scarred" eigenfunctions. The analysis of Eckhardt, Hose, and Pollack [15] in terms of adiabatic stability and a dynamical confining potential provides a better understanding of the complex process. It is now clear that instability of the isolated periodic orbits in the Lyapunov sense (long-time behavior) is not sufficient for the quantum description to alter dramatically. In fact, it would seem that short-time classical effects are more important in quantum mechanics than the overall phase-space structure.

While such an analysis clearly does not hold from systems without any obvious classical analog such as the present case, it is of interest to see whether eigenfunctions with regions of unexpectedly high probability density do exist. It is in this sense that we shall talk of scarred states.

Figure 7 shows a nodal as well as a contour plot of the spin-up component of the 92nd eigenfunction at $R=19.6$ fm. The contours lie predominantly on the z axis ($\rho=0$). Figure 8 shows the spin-down component of an inter-

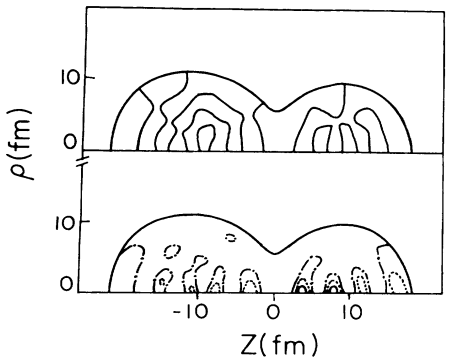

FIG. 7. Scarred state at $R=19.6$ fm, $N=92$, spin up, $E=85.21$ MeV. The localization is along the z axis. The spin-down component is chaotic.

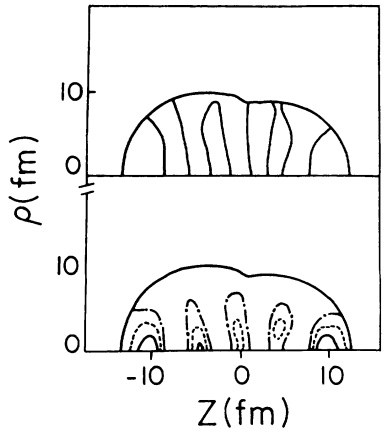

FIG. 8. Scarred state at $R=7$ fm, $N=43$, spin down, $E=61.10$ MeV. The other component is chaotic.

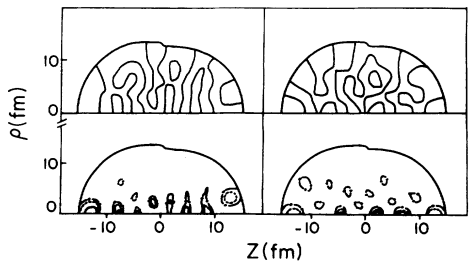

FIG. 9. Nodal and contour plots of the state at $R=4$ fm, $N=109$, and $E=105.98$ MeV. The spin-up component is scarred. The other component is irregular.

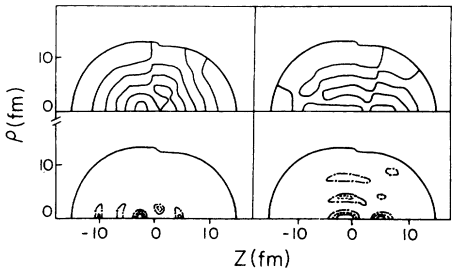

FIG. 10. An example of scarring along both directions. The state is at $R=4$ fm, $N=104$, and $E=101.88$ MeV.

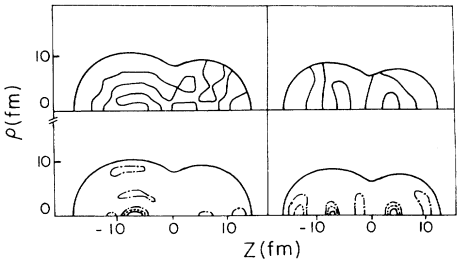

FIG. 11. Nodal and contour plots of the spin-up ($N=77$) and spin-down ($N=37$) components at $R=12$ fm. The eigenenergies are 81.03 and 54.57 MeV, respectively. Both states are scarred.

mediate (43rd) eigenfunction at $R=7$ fm. This is again scarred along the z axis. The other component, however, is irregular in both the cases that we have considered. The phenomenon persists at smaller separations as well. The 109th state at $R=4$ fm is plotted in Fig. 9. Both components seem to be distinctly localized on the z axis though there is a slight spillover in the ρ direction as well. They differ in finer details, however, as in all other cases.

We have also looked for eigenfunctions scarred along the ρ direction. They are relatively fewer in number. The contour and nodal patterns of both components of the 104th eigenfunction at $R=4$ fm are shown in Fig. 10. While the spin-up component is localized on the z axis, the spin-down component shows scarring along the ρ direction. Finally we present (Fig. 11) another example of scarring at intermediate separations ($R=12$ fm). The spin-down component of the 37th state lies on the z axis while the spin-up component of the 77th state is a peculiar instance where the amplitude is distributed along both the z and ρ directions.

Thus scarred states do exist even in systems without any classical limit. The mechanism involved, however, is far from obvious.

V. DISCUSSION

We have carried out a detailed numerical study of the wave functions in the two-center shell model, characterized by the separation R. The presence for the spin-orbit term leads to eigenfunctions which possess two components.

The various criteria used to distinguish regular and irregular states indicate that there is a close overall correspondence between the spectral fluctuations and certain properties of the eigenfunctions. In particular, we have observed the regular-irregular-regular transition (as a function of R) in the nodal and contour plots, a phenomenon observed earlier by Milek, Norenberg, and Rozmej [19] and Pal and Chaudhuri [20] in the spectral fluctuations. In addition, the irregular spatial components were also found to possess a Gaussian amplitude distribution and a few displayed the phenomenon of contour splitting as well, indicating the presence of surface roughness. Thus, even in systems which do not have a clear classical analog, the criteria commonly used to distinguish regular and irregular wave functions do seem to be applicable consistently. Along with the existence of scarred states, we have been able to observe all aspects of wave functions seen in systems with a classical analog.

The presence of scarred wave functions along with the Gaussian amplitude distribution in irregular components give an indication that the semiclassical states are indeed determined by the closed orbits of some effective underlying classical system. Moreover, since the spin-up and spin-down spatial components of each eigenfunction are significantly dissimilar, there seem to be *two sets of closed orbits that give rise to the same spectrum but influence the wave functions in different ways.* We are presently carrying out further investigations along this direction.

[1] M. V. Berry, in *Some Quantum-to-Classical Asymptotics,* 1989 Les Houches Lectures on Chaos and Quantum Physics (North-Holland, Amsterdam, in press).
[2] M. V. Berry and M. Tabor, Proc. Soc. London, Ser. A **356**, 375 (1977).
[3] O. Bohigas, M.-J. Gianonni, and C. Schmit, Phys. Rev. Lett. **52**, 1 (1984).
[4] M. V. Berry, Proc. Soc. London, Ser. A **400**, 229 (1985).
[5] M. V. Berry, in *Stochastic Processes in Classical and Quantum Chaos,* edited by S. S. A. Albeverio, G. Casati, and D. Merlini (Springer, Berlin, 1986).
[6] M. C. Gutzwiller, J. Math. Phys. **11**, 1971 (1970); **12**, 342 (1971).
[7] R. Balian and C. Bloch, Ann. Phys. (N.Y.) **60**, 401 (1970); **64**, 371 (1971).
[8] M. V. Berry and M. Tabor, J. Phys. A **10**, 371 (1977).
[9] J. H. Hannay and A. M. Ozorio de Almeida, J. Phys. A **17**, 3429 (1984).
[10] M. L. Mehta, *Random Matrices* (Academic, New York, 1967).
[11] E. J. Heller, Phys. Rev. Lett. **53**, 1515 (1984).
[12] D. Wintgen and A. Honig, Phys. Rev. Lett. **63**, 1467 (1989).
[13] E. B. Bogomolny, Physica D **31**, 169 (1988).

[14] M. V. Berry, Proc. R. Soc. London, Ser. A **423**, 219 (1989).
[15] B. Eckhardt, G. Hose, and E. Pollack, Phys. Rev. A **39**, 3776 (1989).
[16] D. Biswas, M. Azam, and S. V. Lawande, Phys. Lett. A **155**, 117 (1991).
[17] M. V. Berry, J. Phys. A **10**, 2083 (1977).
[18] D. Biswas, M. Azam, and S. V. Lawande, J. Phys. A (to be published).
[19] B. Milek, W. Norenberg, and P. Rozmej, Z. Phys. A **334**, 233 (1989).
[20] S. Pal and A. K. Chaudhuri, Nucl. Phys. **A537**, 237 (1992).
[21] A. Lukasiak, W. Cassing, and W. Norenberg, Nucl. Phys. **A426**, 181 (1984).
[22] J. Maruhn and W. Greiner, Z. Phys. A **251**, 431 (1972).
[23] S. W. McDonald and A. N. Kaufman, Phys. Rev. A **37**, 3067 (1988).
[24] E. J. Heller, in *Quantum Chaos and Statistical Nuclear Physics,* edited by T. H. Seligman and H. Nishioka, Lecture Notes in Physics Vol. 263 (Springer-Verlag, Berlin, 1986).
[25] D. Biswas and S. R. Jain, Phys. Rev. A **42**, 3170 (1990).